DISCRETE CHANNEL APODIZATION METHOD

FOR THE ANALYSIS OF HIGH-ENERGY X-RAY DATA.

by

JAIME GUILLERMO CARBONELL

Submitted in Partial Fulfillment

of the Requirements for the

Degree of Bachelor of Science

at the

MASSACHUSETTS INSTITUTE OF TECHNOLOGY

June, 1975

Signature of Author..
Department of Physics, May 5, 1975

Certified by..
Thesis Supervisor

Accepted by..
Chairman, Departmental Committee on Theses

DISCRETE CHANNEL APODIZATION METHOD

FOR THE ANALYSIS OF HIGH-ENERGY X-RAY DATA

by

JAIME GUILLERMO CARBONELL

Submitted to the Department of Physics on May, 1975 in partial fulfillment of the requirements for the degree of Bachelor of Science.

ABSTRACT

The discrete channel apodization method to unfold detected x-ray energy spectra is derived for a detector with a Gaussian response function. Other processes required to determine the true source spectrum at the top of the atomosphere are described. A successful computer implementation, with sample results of the spectral determination process, including the discrete channel apodization method, is presented.

Thesis Supervisor: Dr. Anton Scheepmaker

ACKNOWLEDGEMENTS

The author wishes to especially thank Dr. Anton Scheepmaker for his help and encouragement as supervisor of this thesis. Thanks are extended to the whole M.I.T. x-ray balloon group for making this work possible. The author is also grateful to Stan Ryckman for his help in programming and to Alan Wadja for helping make the text of this thesis more readable.

TABLE OF CONTENTS

Page

INTRODUCTION.. 3

METHODS OF DETERMINING THE ENERGY SPECTRUM OF X-RAY SOURCES.. 5

STUDY OF THE ABSORPTION, FOLDING AND EFFICIENCY EFFECTS OF THE X-RAY DETECTION PROCESS............. 10

DISCRETE CHANNEL APODIZATION METHOD.................. 17

IMPLEMENTATIONS AND RESULTS OF THE APODIZATION ALGORITHM.. 28

CONCLUSIONS.. 36

APPENDIX - FULL LISTING OF SPECTRA AND ITS SUBROUTINES.. 38

BIBLIOGRAPHY.. 51

LIST OF FIGURES

		Page
Figure 1.1	Count rate plot for Crab Nebula drift scans	6
Figure 2.1	X-ray escape probability function	13
Figure 2.2	Gaussian response function folding	14
Figure 2.3	Pulse shape discriminator efficiency function	15
Figure 3.1	Folding of discrete channel x-ray spectrum	18
Figure 3.2	Functions that represent Gaussian folding convolutions	23
Figure 3.3	Extrapolation of detected spectrum	25
Figure 4.1	Tabulation of results printed by SPECTRA	30
Figure 4.2	Tabulation of discrete channel apodization results printed by GAUS	31
Figure 4.3	Graphical representation of spectral determination processes	32
Figure 4.4	Determination of Crab Nebula x-ray energy spectrum	34
Figure 4.5	Crab Nebula spectrum	35

INTRODUCTION

X-ray astronomy is a new and rapidly developing branch of Astronomy. X-ray telescopes, which must be lifted to stratospheric heights or beyond because of the opacity of the atmosphere to x-rays, provide the means of observing celestial x-ray sources. The analysis of the x-ray observation data frequently culminates in the determination of the x-ray energy spectrum for the observed celestial source. The determination of the spectrum is essential to the theoretical study and modeling of the natural phenomena which produce the x-rays.

In order to determine the x-ray spectrum, the observation mechanism must be well understood, and all distorting effects must be fully accounted for. X-ray detectors have a response function which is convoluted (i.e., folded) with the energy spectrum in the detection process. The logical way to determine the spectrum impingent on the detector is to unfold the detected spectrum; unfortunately, this is no simple process. The general problem of reversing the effects of a response function is known as apodization. The theme of this dissertation is the development of an apodization algorithm which may be applied to the phoswich x-ray detector system used by the M.I.T. x-ray balloon group. The discrete channel apodization method is such an algorithm, generally applicable to the class of detector systems which have Gaussian response functions and discrete channels.

The high energy x-ray telescope system cited and described in this investigation was flown to 130,000 feet on a stratospheric balloon by the x-ray balloon group of the M.I.T. Center for Space Research on June, 1974. The telescope system consists primarily of two detector banks of phoswich type x-ray detectors, and associated electronics.

The observed x-ray sources were the Crab Nebula and the Coma and Perseus clusters of galaxies. The sources were observed by the drift-scan method.

METHODS OF DETERMINING THE ENERGY SPECTRUM OF X-RAY SOURCES

The determination of the true spectrum of a celestial x-ray source involves several areas of investigation. For a balloon borne x-ray telescope these areas may be categorized as follows: The measured source spectrum must be determined; i.e., the source and background x-ray fluxes as functions of energy must be separated. Secondly, non-linear efficiency effects of the electronic pulse height analysis must be accounted for in order to determine the spectrum at the detector level. Thirdly, the convolution of the response function with the spectrum impingent on the detector, known as the folding process, must be considered. Finally, there is energy dependent atmospheric attenuation and some attenuating effects in the telescope system which must be taken into account.

The drift scan method of observing an x-ray source facilitates the separation of source and background fluxes.[1] Since the diurnal motion of the Earth causes the celestial sphere to rotate at a constant rate with respect to Earth based coordinates, the telescope can be aimed just ahead of the x-ray source which will drift through the field of view. This observation method is known as a drift scan. If the aspect of the balloon borne system is known, the increase in x-ray count rates, pro-

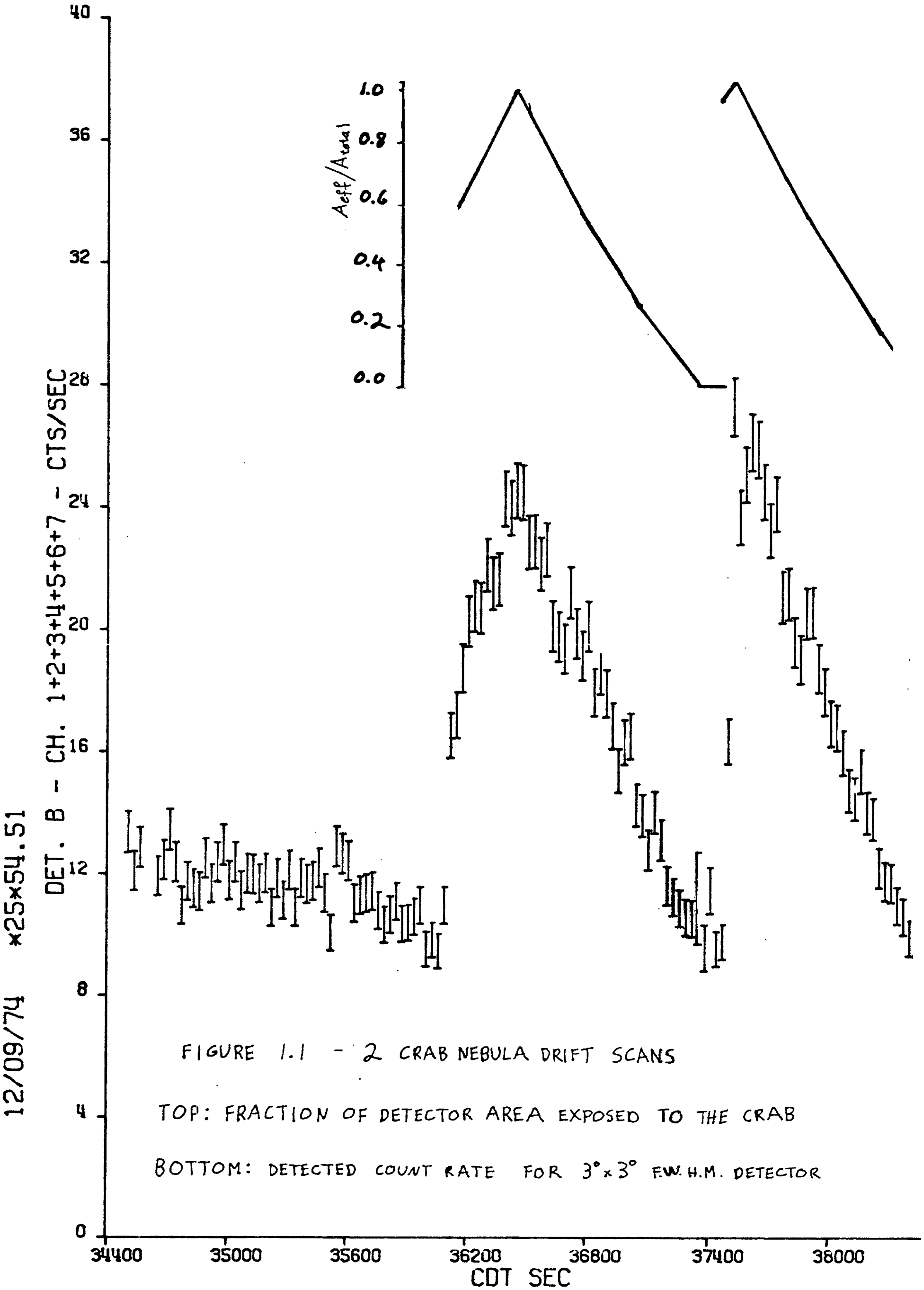

FIGURE 1.1 - 2 CRAB NEBULA DRIFT SCANS

TOP: FRACTION OF DETECTOR AREA EXPOSED TO THE CRAB

BOTTOM: DETECTED COUNT RATE FOR $3° \times 3°$ F.W.H.M. DETECTOR portional to the increase in detector area exposed to the source, can be used to calculate the source intensity (Fig. 1.1). A straight line least squares fit to the x-ray count rate as a function of the detector area may be applied to different energy ranges. Extrapolating the lines, if necessary, to full exposure and to zero exposure yields the full source plus background, and the background count rates respectively (Ryckman, 1974). The background can be independently determined by extending the scan to include a section where no part of the detector is exposed to the source.

The other areas of investigation constitute the determination of the unperturbed source spectrum from the detected spectrum. If all of the attenuating and perturbing effects of the atmospheric absorbtion of the x-rays, folding in the phoswich detectors, and electronic pulse height analysis could be sequentially reversed, then the true spectrum at the top of the atmosphere could be easily determined. This is not the case because the spectrum impingent on the NaI crystal of the phowsich detectors is folded with the detector response function, a process which is not directly reversible.

Most of the X-ray Astronomy research groups use a repeated trial method to converge on a function which closely approximates the true source spectrum.[2] This process requires the critical assumption that the yet unknown source spectrum is best approximated by the theoretically predicted spectral functions. The three types of functions most often postulated by theoretical models of x-ray emitting mechanisms are:[3]

(1.1)

a) $\frac{dN}{dE} = \beta\, E^{-\alpha}$ power law – synchrotron radiation

b) $\frac{dN}{dE} = \frac{Ce^{-E/KT}}{E}$ exponential – bremsstrahlung

c) $\frac{dN}{dE} = \frac{CE^2}{e^{-E/KT} - 1}$ black body radiation

In the repeated trial method one function is selected and the free parameters (e.g., α and β for the power law spectrum) are estimated to generate a trial spectrum. The attenuating and folding effects are applied to the trial spectrum in order to compare it to the detected spectrum. The closeness of the match is usually evaluated under a χ^2 criterion. Next, the free parameters are altered and the spectrum generation process is reiterated in order to minimize χ^2. Often, after many iterations to find the best parameters to fit one function, the entire process is repeated for other theoretically feasible functions.

The repeated trial method has two clear disadvantages over the direct determination of the spectrum at the top of the atmosphere by apodization of the response function and reversing the attenuating processes. Repeated trials are computationally inefficient, and the number of trials required to find an optimal fit to a given function explodes combinatorically as the number of free parameters increases. There are algorithms to generate reasonable guesses for the new values of the free parameters for subsequent trials given the results of previous trials, but these algorithms are computationally costly and dependent on the form of the spectral function being approximated. The other major disadvantage of the repeated trial method is that the choice of approximating function is constrained to simple, theoretically predicted, trial spectra. It is conceivable that more than one mechanism, including the possibility of some absorbtion mechanism, may be operating simultaneously to generate the observed spectrum.

An apodization method that can be implemented and used efficiently avoids the aforementioned difficulties; it avoids the problem of guessing trial spectra and the combinatorial inefficiency of repeated trials with a moderate number of free parameters.[4] The apodization method for discrete channels will be discussed in detail after the different attenuation and pertubation effects are presented.

STUDY OF THE ABSORPTION, FOLDING AND EFFICIENCY EFFECTS OF THE X-RAY DETECTION PROCESS

This section will investigate each process in the sequence of events which a primary x-ray undergoes on its way to the detector, in the detection process, and in the subsequent pulse height analysis. A brief description of the x-ray telescope system for the June 1974 flight should put these processes in their proper perspective.

A) Description of the Detector.

The high-energy x-ray telescope system consists of two detector banks. Each bank consists of four phoswich type x-ray counters behind a slat collimator. For the June flight, one collimator had a $6^{\circ} \times 6^{\circ}$ full width at half maximum (FWHM) field of view, and the other a $3^{\circ} \times 3^{\circ}$ FWHM field of view. The phoswich detectors have a primary 3mm thick NaI crystal coupled to a 1.6" thick CsI secondary crystal. A plastic scintilliation veto counter surrounds the detector banks to reject charged particles. There is an on-board pulse height analysis and telemetry system.[5]

B) Atmospheric Absorption.

The detector system was lifted above 99% of the Earth's atmosphere by a stratospheric balloon, since the opacity of the atmosphere to x-rays prevents them from penetrating substancially deeper. Even in the tenuous stratosphere, x-rays are absorbed as a function of x-ray energy and air thickness traversed. The probability that an x-ray will not be absorbed, called the transmission probability, is given by:

$$(2.1) \qquad P_{TR-AIR}(\mu_A, E) = e^{-\left[5.30\left(\frac{10}{E}\right)^{2.90} + .16\right]\mu_A}$$

where E = x-ray energy in KeV and μ_A = thickness of air traversed measured in gm/cm^2. Air thickness in the zenith direction is a tabulated function of altitude. To calculate the air thickness in the observation direction, the zenith air thickness is mutliplied by the cosecant of the zenith angle of the collimator x-ray axis.

C) Styrofoam Absorption.

There is a protective styrofoam layer above the detectors which abosrbs a small fraction of the x-ray flux as a function of energy. The transmission probability function is simpler than the one for air because of the macroscopically homogeneous nature of styrofoam. The transmission probability is:

$$(2.2) \qquad P_{IR-INS}(E) = e^{-\left(\frac{8.6}{E}\right)^{2.69}}$$

D) Detection Efficiency.

Since the NaI crystal has finite thickness, there is a probability that some x-rays will penetrate the full thickness of the crystal without being detected. In this case the probability that the x-ray is not lost (i.e., detected) is the absorption probability given by

$$(2.3) \qquad P_{AB\text{-}NaI}(\mu_{NaI}, E) = 1 - e^{-A(E)\mu_{NaI}\left(\frac{33}{E}\right)^{2.65}}$$

where μ_{NaI} = thickness of the NaI crystal (= 1.17 gm/cm^2 for a 3mm NaI crystal), and

$$A(E) = \begin{cases} 5.8 & \text{if } E \leq 33 \text{ KeV} \\ 28.0 & \text{if } E > 33 \text{ KeV} \end{cases}$$

The difference in values for $A(E)$ occurs because of the K absorption edge of Iodine at 33 KeV.

E) Escape Probability.

An impingent x-ray whose energy is greater than 33 KeV may excite a K electron in Iodine, giving up 33 KeV's of energy. X-rays are re-emitted when an electron, usually an L state electron, falls into the empty K state. Since x-rays are re-emitted isotropically, there is a theoretical probability that some may escape through the front surface of the NaI crystal. The vast majority of x-rays are detected near the front surface of the 3mm crystal; hence, the probability of escape through the back surface is negligible. The average energy of the re-emitted x-rays is 29.2 KeV. The escape probability as a function of x-ray energy is given in Figure 2.1.

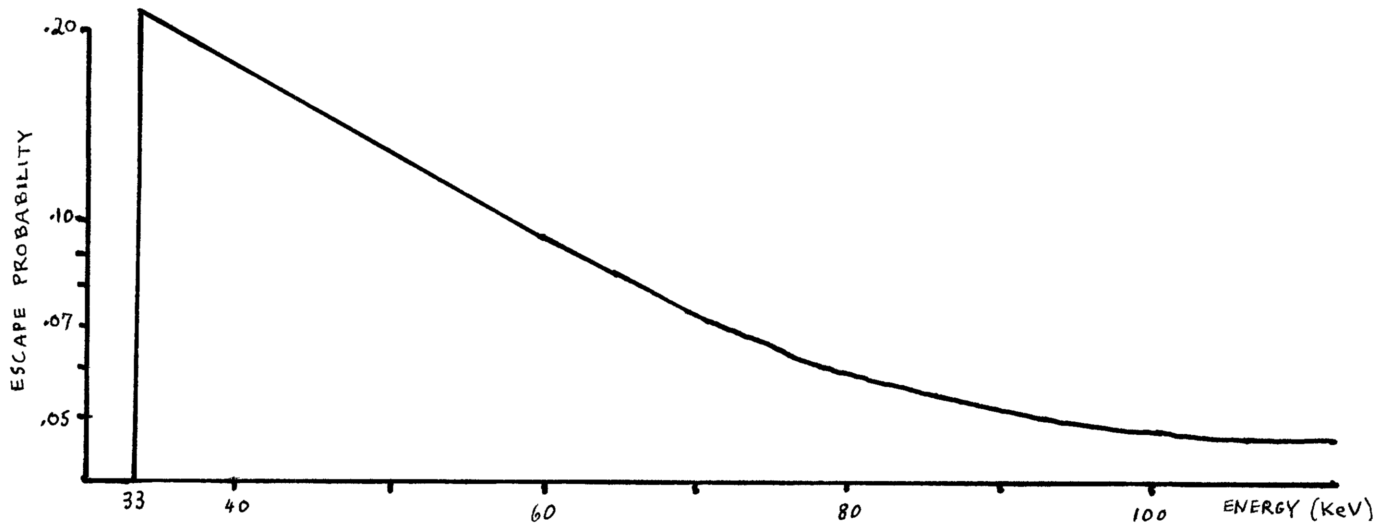

(Fig 2.1) Theoretical probability that an x-ray impingent of a 3 mm NaI crystal will produce an Iodine K-flourescent escape x-ray.

F) Detector Response Function Folding.

In the process of detection in a phoswhich type detector, the impingent x-ray energy spectrum is folded with the response function of the detector to create the detected pulse height spectrum. Let $S(E)$ and $S'(E)$ represent the x-ray energy spectrum, and the pulse height spectrum respectively. $S'(E) = S'(h(H))$ where $h(H)$ is the calibration function that assigns to each pulse height the corresponding energy it represents. The general folding process takes the form:

(2.4) $$S'(E) = \frac{d}{dE} \int S(E)\, G(E)\, dE$$

where $G(E)$ is the response function. Since

$$(2.5) \qquad S(E) = \frac{dN(E)}{dE}\ , \qquad S'(E) = \frac{dN'(E)}{dE}\ ,$$

equation (2.5) can be expressed as:

$$(2.6) \qquad N'(E) = \int E(E)\ dN(E)$$

where $N(E)$ is the number of x-ray counts of energy E per cm^2sec KeV (i.e., the x-ray flux as a function of energy). The response function for a phoswich type detector is a Gaussian, therefore the probability that an x-ray, whose impingent energy is E_o, is detected as having energy between E_1 and E_2 is given by:

$$(2.7) \qquad P_d(E_1 < E < E_2) = \frac{1}{\sqrt{2\pi}\,\sigma(E_o)} \int_{E_1}^{E_2} e^{-(E-E_o)^2/2\sigma(E_o)^2}\, dE$$

where E_o is the mean and $\sigma(E_o)$ is the standard deviation (Figure 2.2).

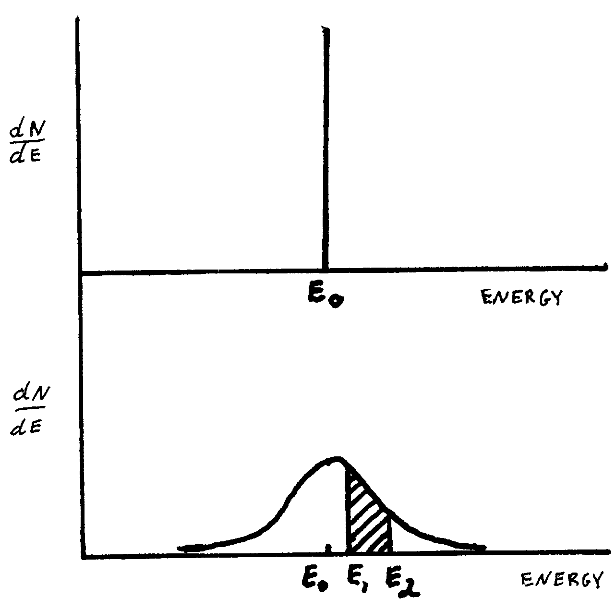

(Fig 2.2) Folding effect. X-ray with impingent energy E_o (δ function) has a probability of being detected between E_1 and E_2 = shaded area under Gaussian response function.

G) Pulse Shape Diserminator Efficiency.

The pulse shape discriminator (PSD) is an electronic system which selects pulses according to the rise time and pulse height. Its efficiency in admitting the appropriate pulses varied (June 1974) as a function of temperature and pulse height during the flight. Therefore, the efficiency had to be determined by an analysis of source calibrations taken during the flight (Scheepmaker, 1974). A source calibration consists of exposing the detectors to an x-ray source of known intensity for a few seconds. Figure 2.3 is the best determination of the efficiency function of the PSD for the June, 1974 flight.

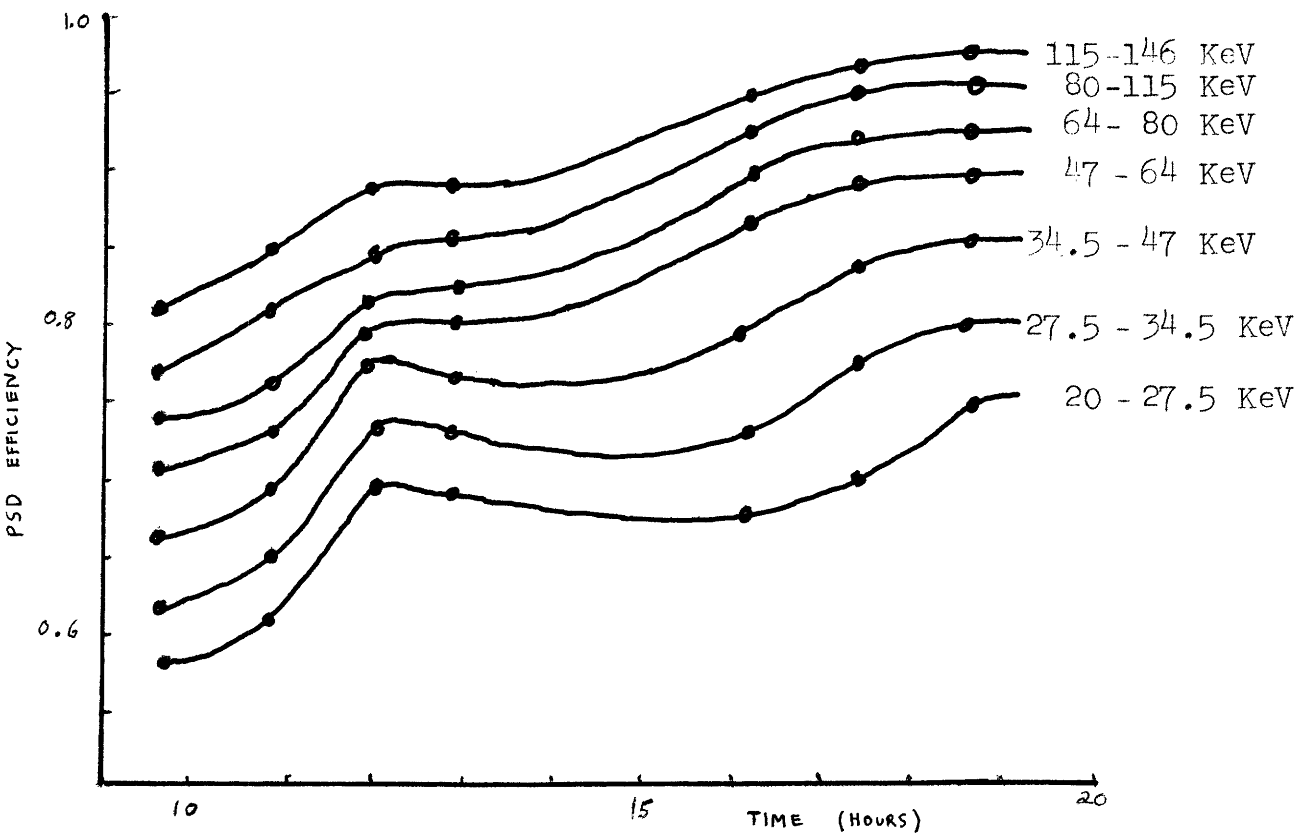

(Fig 2.3) PSD efficiency as a function of time for each energy channel

H) Pulse Height Analyzer.

The pulse height analyzer (PHA) bins the detected x-rays according to energy into discrete pulse height channels. Hence, the spectral data consists of x-ray count rates per pulse height channel. If some of the channel boundaries in the PHA are not well defined, $dN'(E)/dE$ is folded with the boundary resolution functions.

From the mathematical models presented in this section it is evident that all the processes, except for folding, are easily reversible. The following section will analyze an approximation method to reverse the folding process.

DISCRETE CHANNEL APODIZATION METHOD

Discrete channel apodization is the process of unfolding the effects of a response function on a finite number of discrete channels whose energy width is greater than the minimum resolution of the detection system. In this section a mathematical formulation of the folding process is examined and an algorithm for inverting the process is derived. This algorithm, implemented in a spectrum determination program, has proven successful in unfolding detected continuous spectra.

The uncertainty factor in the analysis of discrete channel spectral representations is that no direct determination can be made of the x-ray energy distribution within a single channel. Therefore, for an arbitrary impingent spectrum, a uniform distribution within each channel is assumed, giving the spectrum a characteristic step function. For a system with N energy channels (Fig. 3.1) let (E_i, E_{i+1}) represent the i^{th} channel, i.e., the energy range $\{E \mid E_i < E < E_{i+1}\}$. $\bar{E}_i$ is the energy at the center of the i^{th} channel; $\bar{E}_i = (E_i + E_{i+1})/2$. The indices i and j are assumed to run from 1 to N ($N = 7$ for the June 1974 balloon flight system). $S(\bar{E}_i)$ and $S'(\bar{E}_i)$ represent, respectively, the values of the impingent and detected (unfolded and folded) spectra in of the i^{th} channel.

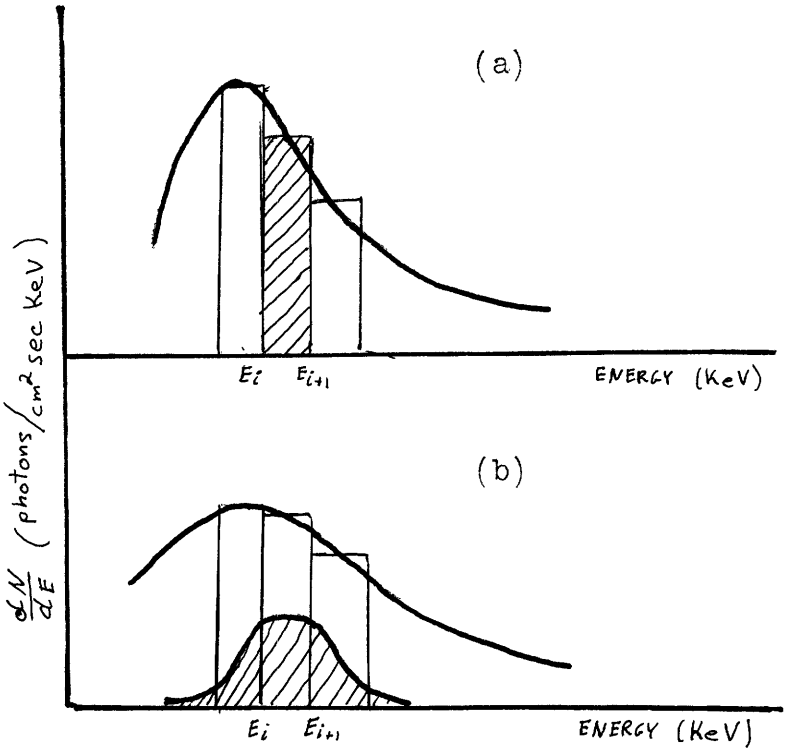

(Fig. 3.1) Folding of discrete channel x-ray spectrum. X-ray flux represented by shaded area in (a) is folded into shaded area in (b) by Gaussian response function.

The response function of the phoswich x-ray detector is a typical Gaussian distribution:

$$(3.1) \qquad G(\bar{E}_j, E) = e^{-(E-\bar{E}_j)^2 / 2\sigma(\bar{E}_j)^2}$$

where

$$(3.2) \qquad \int_{E=-\infty}^{\infty} G(\bar{E}_j, E)\,dE = \sqrt{2\pi}\,\sigma(\bar{E}_j) .$$

$\overline{E}_j$ is the mean of the distribution and $\sigma(\overline{E}_j)$ the standard deviation. $\sigma(\overline{E}_j)$ is calculated empirically from calibration data taken from x-ray line emission sources before the balloon flight (Scheepmaker, 1974). The form of $\sigma(\overline{E}_j)$ may be estimated to within the limits of experimental accuracy by:

$$\sigma(\overline{E}_j) = A \cdot \overline{E}_j + B \cdot \sqrt{\overline{E}_j} + C \tag{3.3}$$

where A, B and C are constants.

Normalizing (3.1) gives a probability distribution function similar to equation (2.7):

$$P_d(E_i < \overline{E}_j < E_{i+1}) = \frac{1}{\sqrt{2\pi}\,\sigma(\overline{E}_j)} \int_{E_i}^{E_{i+1}} G(\overline{E}_j, E)\,dE \tag{3.4}$$

This formulation allows the detected spectrum to be expressed as a step function of the impingent spectrum and the response function for each channel:

$$S'(\overline{E}_i) = \sum_{j=1}^{N} S(\overline{E}_j) \frac{1}{\sqrt{2\pi}\,\sigma(\overline{E}_j)} \int_{E_i}^{E_{i+1}} G(\overline{E}_j, E)\,dE \tag{3.5}$$

$$i = 1,2,\ldots,N$$

The goal of this section is to derive $S(\bar{E}_i)$ from $S'(\bar{E}_i)$, hence reversing the folding process of the response function $G(\bar{E}_j,E)$. The apodization method is usually an approximating process converging to a best approximation of the impingent spectrum.[6] In the present apodization scheme the algorithm simply involves solving a set of N linear equations in N unknowns. Since $G(\bar{E}_j,E)$ is directly computable, (3.5) yields a system of linear equations with unknowns $S(\bar{E}_j)$ for a given set of $S'(\bar{E}_i)$. Letting

$$(3.6) \qquad [a_{ij}] = \left[\frac{1}{\sqrt{2\pi}\ \sigma(\bar{E}_j)} \int_{E_i}^{E_{i+1}} G(\bar{E}_j,E)\,dE \right]$$

be the coefficient matrix, (3.5) takes the form:

$$(3.7) \qquad [a_{ij}]\ [S(\bar{E}_j)] = [S'(\bar{E}_i)]\ .$$

Since $[a_{ij}]$ is nonsingular and diagonally dominant, there exists a straightforward solution procedure for the $S(\bar{E}_j)$.

The aforementioned apodization algorithm makes four simplifying assumptions to the general apodization problem. Two of the assumptions are imposed by the detector system:

the finite number of discrete channels and the Gaussian response function. The other assumptions are approximations to simplify the mathematical analysis. The uniform distribution within each channel is an assumption which does not introduce significant inaccuracies. The development of an apodization method which does not require this assumption will be discussed at the end of this section. The fourth assumption is implicit in (3.4) where the probability of detection is calculated to be a single Gaussian distribution centered about the mean $\overline{E}_j$. This assumes that the uniform distribution inside the j^{th} channel may be considered a delta function at the mean, an assumption which is good only if the channel width is small with respect to the standard deviation, $\sigma(E_j) >> E_{j+1} - E_j$.

For the June 1974 detector system the channels are wide with respect to the standard deviation. Given a uniform x-ray flux for the i^{th} channel, the exact form of the convolution with the Gaussian response function for the j^{th} channel is:

$$P_j(E) = \int_{E_j}^{E_{j+1}} U(E_j, E_{j+1})\, G(E, E')\, dE'$$

(3.8)

$$= \frac{1}{(E_{j+1} - E)\sqrt{2\pi}\,\sigma(\overline{E}_j)} \int_{E_j}^{E_{j+1}} e^{-(E-E')^2/2\sigma(\overline{E}_j)^2}\, dE'$$

Therefore, the probability that an x-ray impingent on the j^{th} channel is detected at the i^{th} channel is the definite integral of (3.8) over the i^{th} channel:

$$
\begin{aligned}
P_{d_j}(E_i \le E < E_{i+1}) &= \int_{E_i}^{E_{i+1}} P_j(E)\,dE = \frac{1}{(E_{j+1}-E_j)\sqrt{2\pi}\,\sigma(\bar{E}_j)} \\
&\times \int_{E_i}^{E_{i+1}} \int_{E_j}^{E_{j+1}} e^{-(E'-E)^2/2\sigma(\bar{E}_j)^2}\, dE'\,dE
\end{aligned}
\tag{3.9}
$$

The exact expression for the total flux detected in the i^{th} channel is:

$$
\begin{aligned}
S'(\bar{E}_i) &= \sum_{j=1}^{N} \frac{S(\bar{E}_j)}{(E_{j+1}-E_j)\sqrt{2\pi}\,\sigma(\bar{E}_j)} \\
&\times \int_{E_i}^{E_{i+1}} \int_{E_j}^{E_{j+1}} e^{-(E'-E)^2/\sigma(\bar{E}_j)^2}\, dE'\,dE
\end{aligned}
\tag{3.10}
$$

$$i = 1,2,\ldots,N$$

which is a system of linear equations. (3.10) may be represented in the same form as (3.7) and solved by inverting the coefficient matrix. In the limit as $(E_{j+1}-E_j) \to 0$ (3.9) is equivalent to (3.4); hence, as previously stated, the first apodization algorithm is valid for very narrow energy channels.[7]

Solving the system of equations (3.10) proved to be impractical in terms of computer time required to generate the coefficient matrix. The numerical evaluation of

$$(3.11) \qquad D_{ij} = \int_{E_i}^{E_{i+1}} \int_{E_j}^{E_{j+1}} e^{-(E'E)^2/2\sigma(\bar{E}_j)^2}\, dE'dE$$

by iterative application of numerical integration techniques is somewhat costly, and there are N^2 ($N^2 = 49$ for the present system) D_{ij} to evaluate. A more efficient method of calculating the D_{ij} has recently been found, after an approximating system of equations equivalent to (3.10) was programed and used in the data analysis.

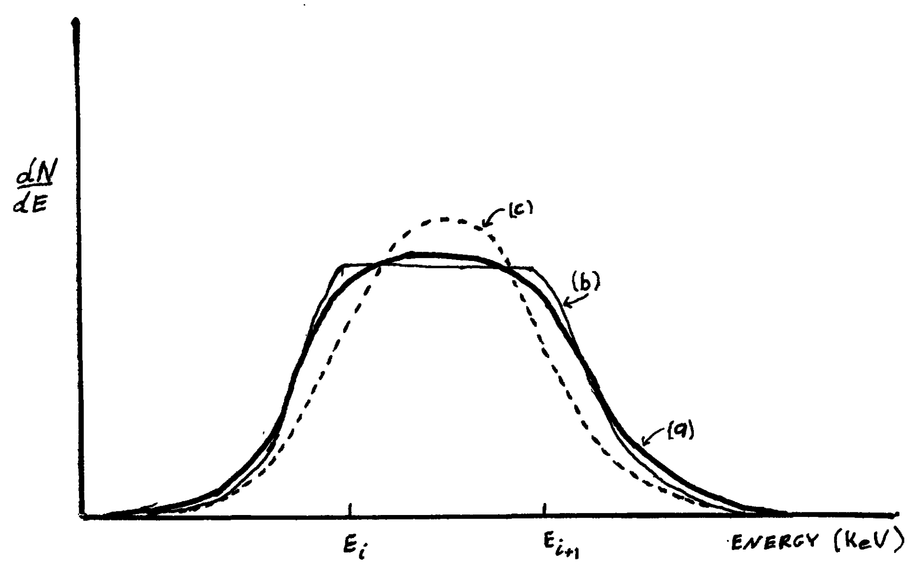

(Fig 3.2) Folded channel function for a) exact form of Gaussian response convoluted with uniform distribution, b) close numerical approximation to (a), c) single Gaussian, considering x-ray flux to be δ function at center of channel.

Equation (3.9) may be approximated by minimizing the L_1 norm of the concatentation of two half Gaussians and a constant function (Fig. 3.2). The probability that an x-ray impingent in the j^{th} channel is detected at the i^{th} channel becomes:

$$P_{dj}(E_i<E<E_{i+1}) = \begin{cases} \dfrac{1}{\sqrt{2\pi}\,\sigma(E_j)+(E_{i+1}-E_i)P_{\alpha i}} \times \displaystyle\int_{E_i}^{E_{i+1}} e^{-(E-E_j)^2/2\sigma(\bar{E}_j)^2}\,dE\,, & \text{if } j<i \\ P_{\alpha j}\,, & \text{if } j = i \\ \dfrac{1}{\sqrt{2\pi}\,\sigma(E_j)+(E_{i+1}-E_i)P_{\alpha i}} \times \displaystyle\int_{E_i}^{E_{i+1}} e^{-(E-E_{j+1})^2/2\sigma(\bar{E}_j)^2}\,dE\,, & \text{if } j>i \end{cases} \tag{3.12}$$

For $i = 1,2,\ldots,N$

where $P_{\alpha j} = 1 - \sum_{j \neq i} P_{dj}(E_i < E < E_{i+1})$ is the probability that an x-ray impingent on the j^{th} channel is detected in the j^{th} channel. In this approximation the respective means of the Gaussians are at the channel boundaries, making the derivative of the approximating function well defined and everywhere continuous.

The detected spectrum on the i^{th} channel can be expressed as a sum of the impingent spectrum multiplied by the respective detection probabilities, as in the previous methods:

$$S'(\overline{E}_i) = \sum_{j=1}^{N} S(\overline{E}_j)P_{dj}(E < E < E_{i+1}) \tag{3.10}$$

$$i = 1,2,\ldots,N$$

The system of linear equations may then be solved for $S_\alpha(\overline{E}_j) = S(\overline{E}_j)P_{\alpha j}$, which yields $S(\overline{E}_j)$ directly. $S_\alpha(\overline{E}_j)$ is called the alpha spectrum; it is the fraction of the spectrum in each channel not carried to a different channel by the response function.

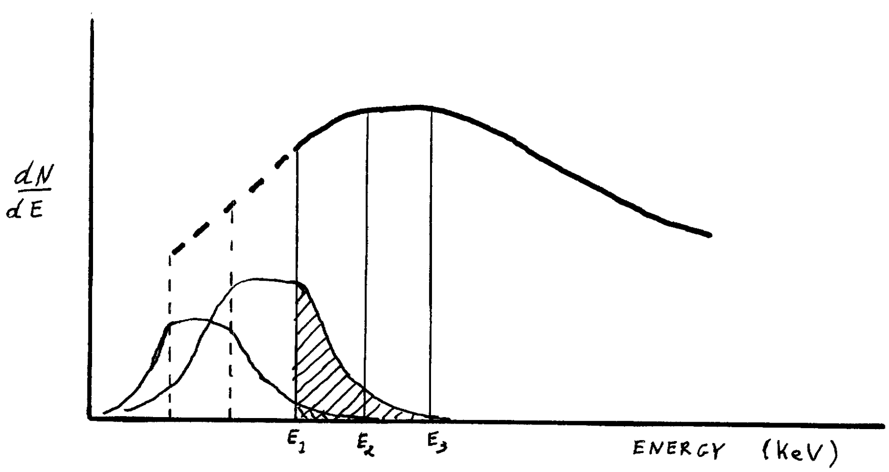

(Fig 3.3) Extrapolation of detected spectrum to estimate the fraction of the flux folded into the extreme channels from x rays whose impingent energy lies beyond the threshold of the extreme channel boundaries.

There is a non-negligible probability that x-rays impingent with slightly less energy than the lowest energy channel boundary, or with energy slightly higher than the highest channel boundary, will be folded into the respective extreme channel by the response function. Likewise, a fraction of the impingent flux at the extreme channels is never detected; it is carried out of detection range by the Gaussian response (Fig. 3.3). In order to minimize errors caused by ignoring this effect, the detected spectrum is extrapolated beyond the energy range of the extreme channels. A reasonable extrapolation will yield correction estimates for the x-ray fluxes carried across the extreme boundaries.

At the time of this writing the development of a more accurate, but also more complicated, method is being investigated. This method determines a smooth, best L_2 - approximate to the detected spectrum. The process assigns to each $\bar{E}_i$ a tentative $\left.\frac{d}{dE} S'(E)\right|_{E=\bar{E}_i}$ and a somewhat more tentative $\left.\frac{d^2}{dE^2} S'(E)\right|_{E=\bar{E}_i}$ in order to give a reasonable approximation to the x-ray distribution within each channel. The approximating functions under investigation are interpolating cubic splines, where the number of splined sections is a function of the number of energy channels. The splining method will give a more accurate determination of the impingent spectrum in systems incorporating a somewhat larger number of energy channels.

IMPLEMENTATION AND RESULTS OF THE APODIZATION ALGORITHM

SPECTRA is a Fortran IV computer program which lifts an x-ray spectrum from the detected count rates in each channel to the true x-ray source spectrum at the top of the atmosphere. An implementation of the discrete channel apodization algorithm lies at the heart of SPECTRA in a subprogram called GAUS.

SPECTRA applies the inverse process of each attenuation or pertubation, previously described, in reverse order from the detection process. Since the apodization algorithm inverts the folding process, a single program run will yield the best values of the source spectrum at a small computational cost. SPECTRA takes as input the set of detector system parameters and the detected count rates per energy channel for each detector bank. The detector parameters are: air thickness, NaI crystal thickness, detector area at full source exposure for each detector bank, time in the flight when the detected count rates were accumulated, PSD efficiency table with efficiency values for different x-ray energies and different times during the flight, and PHA channel boundaries in terms of energy. (Pulse height is directly porportional to energy.)

The count rate in each channel is converted to units of counts/cm^{2}sec KeV . The PSD efficiency table is interpolated to calculate the closest value for each energy channel at the given time in the flight, and the efficiency correction is applied to the spectrum. SPECTRA calls GAUS with the efficiency corrected spectrum to apply the discrete channel apodization algorithm. GAUS, in turn, calls several functions and subroutines, including RSIMQ to solve the linear matrix equation (3.13). (RSIMQ was developed by the Information Processing Center at M.I.T.). After the escape correction is applied to the unfolded spectrum, there follows a sequential application of the corrections for NaI crystal transmission, styrofoam layer absorption, and atmospheric absorption. The resultant step function is the best discrete determination of the continuous x-ray source spectrum at the top of the atmosphere. The spectral step function can be easily χ^2 fitted to a theoretically predicted spectrum (e.g., power law).

SPECTRA tabulates the results at each step in lifting a detected spectrum to the top of the atmosphere (Figure 4.1). GAUS prints out the probability coefficient matrix,

$$(4.1) \qquad [a_{ij}] = P_{dj}(E_i < E < E_{i+1})/P_{\alpha i}$$

and the unfolding of the energy spectrum (Figure 4.2).

In order to test the accuracy of SPECTRA, a close approximation to the Crab Nebula power law spectrum,[8]

UNITS = CTS/(CM**2*SEC*KEV)

ENERGY BIN		MEASURED SP	EFFEL CORR	EFFPSC CORR	NAI UNFOLDING	ESCAPE CORR	NAI ABSORPTION	TRINS	TRAIR(FINAL)
20.00	27.50	1.3510E-03	1.4372E-03	2.4043E-03	2.4926E-03	2.4167E-03	2.4167E-03	2.5861E-03	1.8751E-02
27.50	34.50	1.5723E-03	1.6727E-03	2.6318E-03	2.7511E-03	2.6943E-03	2.6952E-03	2.7868E-03	9.2839E-03
34.50	47.00	1.1965E-03	1.2728E-03	1.8642E-03	1.8719E-03	2.3141E-03	2.3141E-03	2.3519E-03	5.4368E-03
47.00	64.00	8.5248E-04	9.0689E-04	1.2547E-03	1.2762E-03	1.4364E-03	1.4367E-03	1.4471E-03	2.7977E-03
64.00	80.00	5.4298E-04	5.7764E-04	7.6734E-04	7.4881E-04	7.9666E-04	8.0949E-04	8.1240E-04	1.4714E-03
80.00	115.00	2.7481E-04	2.9235E-04	3.6748E-04	3.7214E-04	3.8377E-04	4.5487E-04	4.5560E-04	7.9765E-04
115.00	146.00	1.0481E-04	1.1150E-04	1.3345E-04	1.2150E-04	1.2814E-04	2.2262E-04	2.2278E-04	3.8472E-04

TOTAL INTEGRATED FLUX BETWEEN 20.00 AND 146.00KEV IN UNITS OF XRAYS/(CM**2*SEC) IS 3.84525E-01

(Fig 4.1) Tabulation of the results printed by SPECTRA at all stages in the determination of the discrete representation of the x-ray source spectrum at top of the Atmosphere. The results presented herein and graphed in Figure 4.3 are the recovery of a power law spectrum ($\alpha = -2.25$, $\beta = 22$) after modeled detector folding, attenuation and efficiency processes were applied.

UNFOLDING OF SPECTRUM NUMBER 2

AIR THICKNESS = 3.350 GRAMS/CM SQ NAI THICKNESS = 1.170 GRAMS/CM SQ
σ of RESPONSE FUNCTION = 0.030 * ENERGY + 0.420 * SQRT(ENERGY) + 0.230

PROBABILITY CONVOLUTION MATRIX

1.000	0.207	0.000	0.000	0.0	0.0	0.0
0.189	1.000	0.261	0.000	0.000	0.0	0.0
0.000	0.124	1.000	0.178	0.000	0.000	0.0
0.0	0.000	0.108	1.000	0.155	0.000	0.0
0.0	0.0	0.000	0.139	1.000	0.202	0.000
0.0	0.0	0.0	0.000	0.075	1.000	0.113
0.0	0.0	0.0	0.0	0.0	0.104	1.000

ENERGY BIN		FOLDED SPECT	ALPHA SPECT	UNFOLDED SP
20.00	27.50	2.2293E-03	1.8346E-03	2.4826E-03
27.50	34.50	2.6318E-03	1.9066E-03	2.7511E-03
34.50	47.00	1.8642E-03	1.4476E-03	1.8719E-03
47.00	64.00	1.2547E-03	1.0114E-03	1.2762E-03
64.00	80.00	7.6734E-04	5.6311E-04	7.4881E-04
80.00	115.00	3.6748E-04	3.1407E-04	3.7214E-04
115.00	146.00	1.2955E-04	9.6763E-05	1.2150E-04

(Fig 4.2) Discrete Channel Apodization computational results. GAUS prints the $[a_{ij}]$ coefficient probability matrix and the unfolded spectrum. Results tabulated in this run are from the recovery of the power law mentioned in the previous figure.

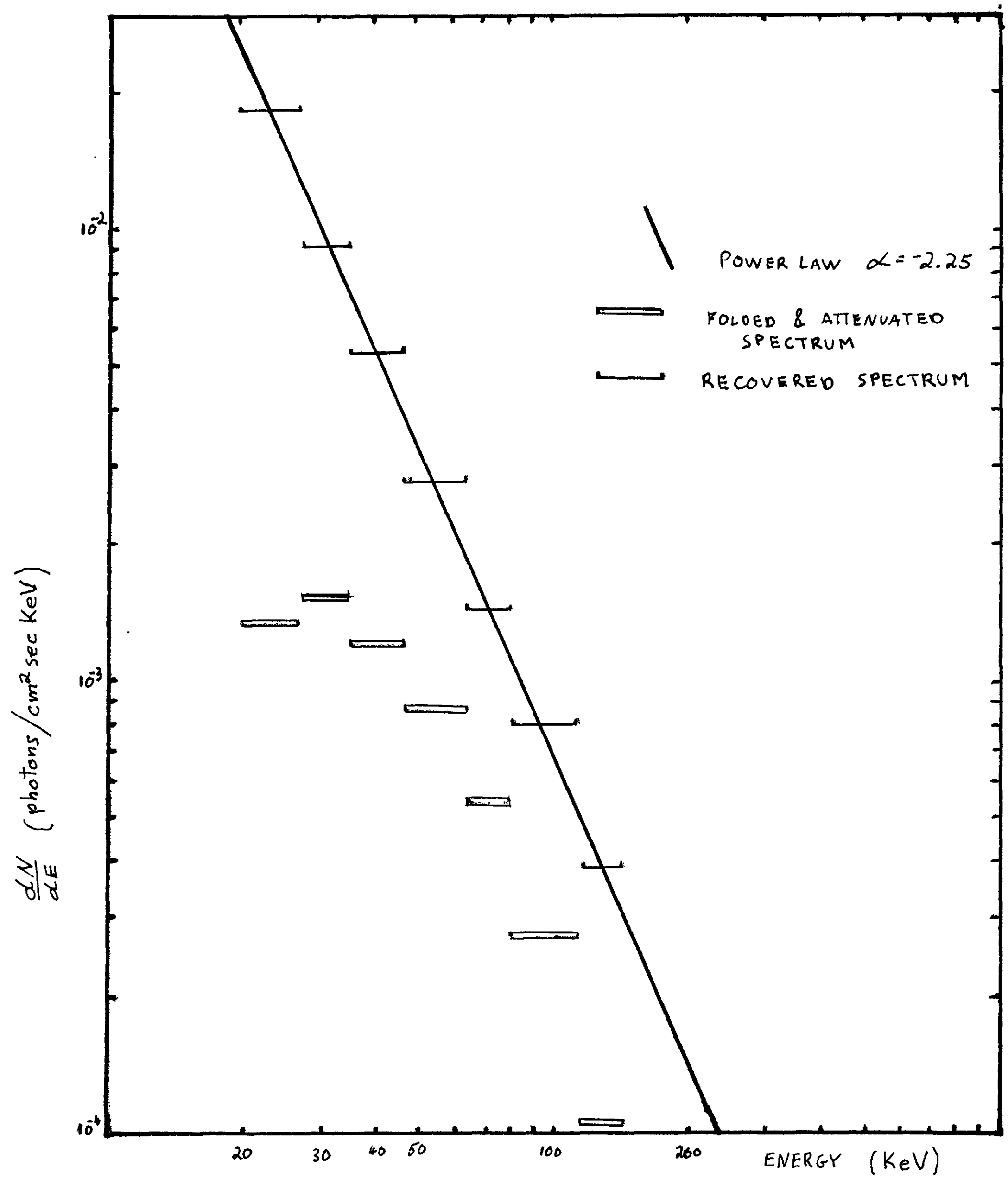

(Fig 4.3) Comparison of **original power law** spectrum, folded, attenuated spectrum, and recovered spectrum by SPECTRA.

$$\frac{dN}{dE} = 22E^{-2.25} \quad \text{(photons/cm}^2\text{sec KeV)} \tag{4.2}$$

was folded with the detector response function, and all other absorption and efficiency effects were applied (Laros, 1973). The resultant spectrum, generated to simulate a detected spectrum, was given to SPECTRA, which recovered the original spectrum at the top of the atmosphere with small computational errors (Fig. 4.1 and 4.3). The highest and lowest energy channels have somewhat larger errors than the central channels due to the extrapolation of the "detected" spectrum necessary to calculate the effects of the response function at the boundaries of the spectrum.

SPECTRA was applied to detected spectra from Crab Nebula drift scans. The result of one computer run, for the second Crab scan in the June, 1974 flight, is presented in Figures 4.4 and 4.5. The second and fourth energy channels are respectively too low and too high with respect to the Laros spectrum. This was found to be the case for other methods of determining the spectrum and for other Crab scans.

SPECTRA was tested for different detector system parameters. For instance, the unfolding of a test spectrum gave more accurate results when 12 energy channels were used to span the 20-146 KeV energy range instead of the 7 channels in the June flight.

UNITS = CTS/(CM**2*SEC*KEV)

ENERGY BIN	MEASURED SP	EFFEL CORR	EFFPSD CORR	NAI UNFOLDING	ESCAPE CORR	NAI ABSORPTION	TRINS	TRAIR(FINAL)
20.00 27.50	1.3922E-03	1.4811E-03	2.4776E-03	2.5780E-03	2.4889E-03	2.4889E-03	2.6633E-03	1.9311E-02
27.50 34.50	1.0500E-03	1.1170E-03	1.7576E-03	1.4989E-03	1.4238E-03	1.4243E-03	1.4727E-03	4.9061E-03
34.50 47.00	1.1205E-03	1.1920E-03	1.7458E-03	1.7736E-03	2.1645E-03	2.1645E-03	2.1998E-03	5.0852E-03
47.00 64.00	1.1208E-03	1.1923E-03	1.6457E-03	1.7385E-03	1.9581E-03	1.9586E-03	1.9727E-03	3.8140E-03
64.00 80.00	7.5118E-04	7.9913E-04	1.0616E-03	1.0644E-03	1.1357E-03	1.1540E-03	1.1581E-03	2.0975E-03
80.00 115.00	3.1365E-04	3.3367E-04	4.1942E-04	4.0690E-04	4.1750E-04	4.9485E-04	4.9565E-04	8.6777E-04
115.00 146.00	1.4857E-04	1.5805E-04	1.8916E-04	1.7390E-04	1.8340E-04	3.1862E-04	3.1886E-04	5.5063E-04

TOTAL INTEGRATED FLUX BETWEEN 20.00 AND 146.00KEV IN UNITS OF XRAYS/(CM**2*SEC) IS 3.88579E-01

(Fig 4.4) Determination of Crab Nebula x-ray energy spectrum. There is close agreement between unfolded spectrum and power law with parameters $\alpha = -2.25$ $\beta = 22$. The Integrated flux between 20 and 146 KeV for the power law is 3.814 E - 1 x-rays/cm^2 sec.

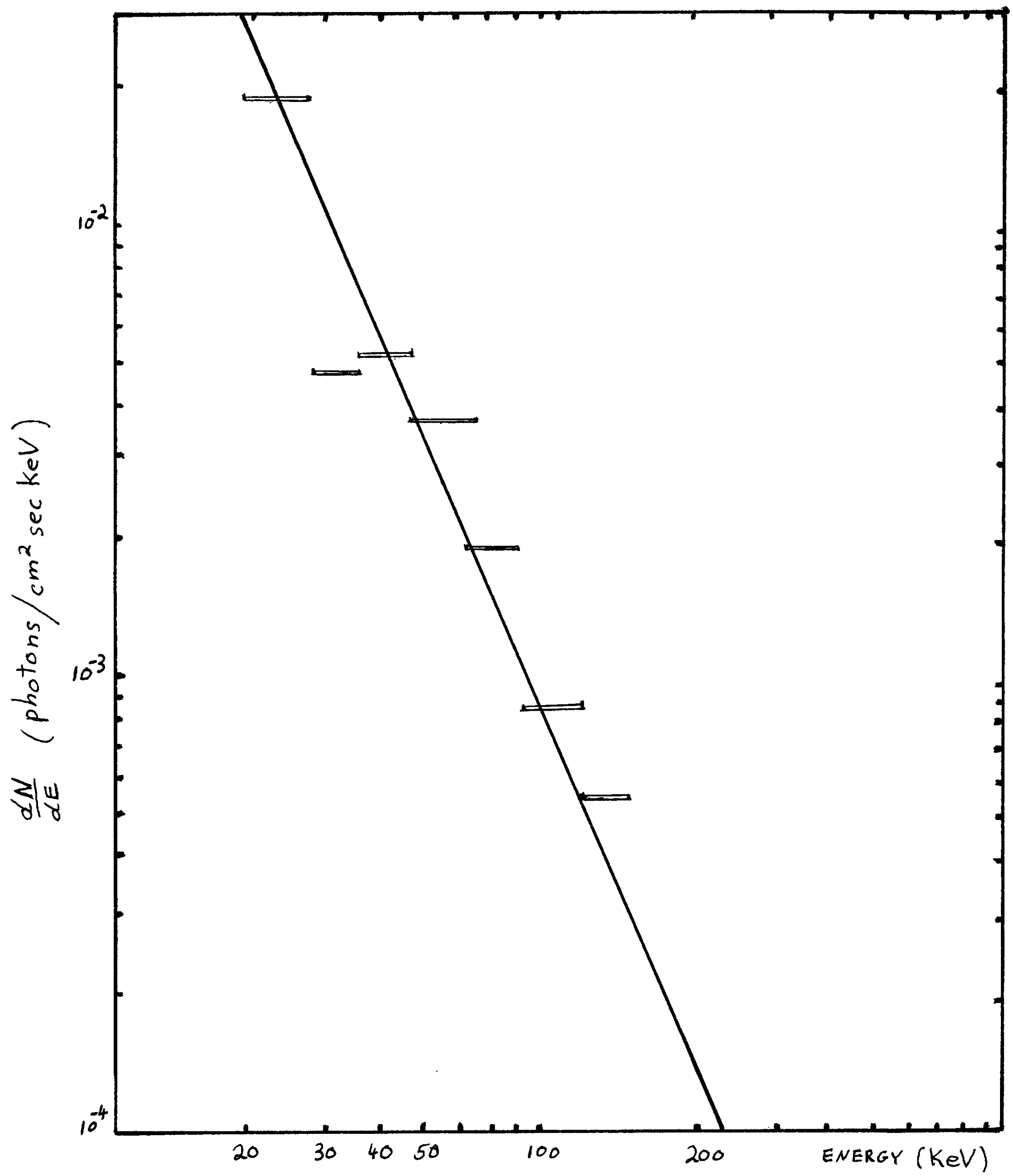

(Fig 4.5) Graphical representation of the determined x-ray energy spectrum for the Crab Nebula. The power law, given as a reference, is the Laros spectrum.

CONCLUSIONS

The discrete channel apodization technique yields the closest obtainable values to the true x-ray source energy spectrum at the top of the atmosphere in a single, efficient pass. These values may be matched to a theoretically predicted spectrum (e.g., under a χ^2 minimization criterion) if one wishes to study the x-ray production mechanism. The calculated values for the source spectrum are independent of any fitting performed after the determination of the spectrum, unlike the repeated trial method, where nothing is known about the source spectrum until a reasonable fit is found. The determination of the source spectral parameters may be greatly facilitated by graphing the source spectrum and performing preliminary visual fitting, or, at least, setting severe constraints on the type of function and values for the free parameters chosen for the χ^2 fit.

The discrete channel apodization algorithm may be applied to any x-ray detector with discrete channels and a Gaussian response function. It may be possible to generalize the method to include other types of response functions, but the necessity for discrete channels lies at the very heart of the algorithm.

There are some limitations to the apodization method. Only continuous spectra can be unfolded; line spectra cannot be resolved by discrete channel apodization. In order to get accurate results for continuous spectra, the detector system needs to have at least five energy channels. On the whole, the discrete channel apodization algorithm is an efficient and fruitful process applied to the determination of the x-ray source spectrum at the top of the atmosphere. The author hopes that this method may be used by x-ray astronomers to facilitate and improve their spectrum determinations.

APPENDIX

FULL LISTING OF SPECTRA AND ITS SUBROUTINES

SPECTRA is a Fortram program which should be compatible with most Fortran IV implementations. The data is read in from a set of cards of specified format, fully explained in the first page of the listing. SPECTRA can process several detected spectra measured during a single balloon flight in one program run.

The discrete channel apodization algorithm is implemented in the subroutine GAUS, which may be used independently of SPECTRA for detector systems that are not balloon borne (e.g. satellite detectors), but which have a Gaussian response function and discrete channels.

```
C-----MAIN PROGRAM TO LIFT BALLOON DETECTED X-RAY SPECTRA TO THE TOP OF
C      THE ATMOSPHERE. ASSUMES DISCRETE CHANNELS AND GAUSSIAN RESPONSE
C      FUNCTION FOR THE DETECTOR
C
C
C-----WRITTEN AT MIT JANUARY THRU APRIL 1975 BY JAIME G. CARBONELL
C
C
C-----REQUIRES 4 SUBROUTINES,
C      1) GAUS = APODIZATION ALGORITHM FOR DISCRETE CHANNELS AND GAUSSIAN RESP.
C      2) RSIMQ SOLVES SYSTEM OF N LINEAR EQUATIONS IN N UNKNOWNS
C      3) ESCAPE INVERTS ESCAPE EFFECT OF IODINE ABSORPTION K EDGE IN NAI X-TAL.
C      4) EPSD CALCULATES EFFICIENCY OF PSD BY INTERPOLATION ON TIME AND ENERGY.
C
C
C-----REQUIRES 9 FUNCTIONS
C      GAUSP  XTRPOL  ESCR  TRAIR  TRNAI  TRINS  SIGF  EFFEL  FINTRP
C
C
C-----FIRST SET OF DATA CARDS IS THE EFFICIENCY TABLE PRECEEDED BY 1 CARD
C      WITH THE (I2) NUMBER OF ENTRIES (= NUMBER OF TIMES IN FLIGHT = NUMBER
C      OF CARDS IN EFFICIENCY TABLE.) EACH CARD CONSISTS OF A TIME IN CCT SEC.
C      FOLLOWED BY 7 EFFICIENCY VALUES, ONE FOR EACH CHANNEL.
C
C
C-----SECOND SET OF DATA CARDS CONSISTS OF DETECTOR PARAMETERS
C      1) NUMBER OF ENERGY CHANNELS  (I2)
C      2) THICKNESS OF NAI CRYSTAL IN GM/CM**2  (F7.3)
C      3) A,B,C VALUES FOR SIGF RESPONSE FUNCTION (3F7.3)
C      4) NBINS+1 ENERGY BOUNDARY VALUES (10F7.2)
C      5) NUMBER OF SPECTRA TO BE PROCESSED (I2)
C-----THE FOLLOWING CARDS APPLY TO EACH SPECTRUM - MUST BE REPEATED
C      6) DETECTOR AREA IN CM**2 (F10.1)
C      7) CCT TIME (F10.1)
C      8) AIR THICKNESS IN GM/CM**2 (F7.3)
C      9) COUNT RATES PER CHANNEL (DETECTED) IN CTS/SEC (10F7.3)
C
C
C
      REAL EKEV(51),EKEVA(50),TSPECT(50),SPECT(50,8)
      REAL SIGVAL(50),SIGPAR(3)
      EFF=1.0
      CALL EPSD
      READ(5,10) NBINS
 10   FORMAT(I2)
      READ(5,11) THNAI
 11   FORMAT(F7.3)
      READ(5,12) (SIGPAR(I),I=1,3)
 12   FORMAT(3F7.3)
      KK=NBINS+1
      READ(5,13) (EKEV(I),I=1,KK)
 13   FORMAT(10F7.2)
      ISPEC=0
      READ(5,14) NSPEC
 14   FORMAT(I2)
 100  IF(NSPEC.LE.ISPEC) GO TO 101
      ISPEC=ISPEC+1
      READ (5,18) AREA
```

```
                READ(5,18) CDTIME
         18     FORMAT(F10.1)
                READ(5,11) THAIR
                READ(5,15) (SPECT(I,1),I=1,NBINS)
         15     FORMAT(10F7.3)
         C-----PRINT OUT INPUT PARAMETERS READ
                WRITE(6,16) ISPEC,THAIR,THNAI,(SIGPAR(I),I=1,3)
         16     FORMAT('1',//////' UNFOLDING OF SPECTRUM NUMBER ',I2,//
               1' AIR THICKNESS =',F7.3,' GRAMS/CM SQ     NAI THICKNESS =',
               2F7.3,' GRAMS/CM SQ',/' RESPONSE FUNCTION =',F7.3,' * ENERGY    +
               1 ',F7.3,' * SQRT(ENERGY)    +  ',F7.3,/////)
                DO 29 J=1,NBINS
         29     EKEVA(J)=(EKEV(J)+EKEV(J+1))/2
                DO 30 J=1,NBINS
                K=J+1
                SPECT(J,1)=SPECT(J,1)/(AREA*(EKEV(K)-EKEV(J)))
                SPECT(J,2)=SPECT(J,1)/EFFEL(EKEVA(J))
                CALL EFFPSC(EFF,CDTIME,EKEVA(J),EKEVA)
                SPECT(J,3)=SPECT(J,2)/EFF
                TSPECT(J)=SPECT(J,3)
         30     SIGVAL(J)=SIGF(EKEVA(J),SIGPAR(1),SIGPAR(2),SIGPAR(3))/2.0
                CALL GAUS(NBINS,EKEV,EKEVA,SIGVAL,TSPECT,SIGPAR)
                WRITE(6,17) (SIGVAL(I),I=1,NBINS)
         17     FORMAT('OSIGVAL=  ',10F7.2)
         C-----NAI CRYSTAL UNFOLDING JUST COMPLETED -- NOW DO FIRST ORDER
         C      ESCAPE CORRECTION AND BRING SPECTRUM TO TOP OF ATMOSPHERE
                TFLUX=0
                DO 41 J=1,NBINS
         41     SPECT(J,4)=TSPECT(J)
                CALL ESCAPE(EKEV,TSPECT,NBINS)
                DO 31 J=1,NBINS
                K=J+1
                SPECT(J,5)=TSPECT(J)
                SPECT(J,6)=SPECT(J,5)/(1.0-TRNAI(THNAI,EKEVA(J)))
                SPECT(J,7)=SPECT(J,6)/TRINS(EKEVA(J))
                SPECT(J,8)=SPECT(J,7)/TRAIR(THAIR,EKEVA(J))
                TFLUX=TFLUX+SPECT(J,8)*(EKEV(K)-EKEV(J))
         31     CONTINUE
         C-----PRINT SPECTRUM AT EACH STEP IN PROCESSING AND UNFOLDING
                WRITE (6,37)
         37     FORMAT('O UNITS = CTS/(CM**2*SEC*KEV)'/)
                WRITE(6,32)
         32     FORMAT('O     ENERGY BIN     MEASURED SP    EFFEL CORR    EFFPSC COR
               1R  NAI UNFOLDING   ESCAPE CORR   NAI ABSORPTION    TRINS     TRAIR(F
               2INAL)')
                DO 34 J=1,NBINS
                K=J+1
                WRITE(6,38)
         38     FORMAT(' I-----------------------------------------------------
               1-----------------------------------------------------------------
               2-------I')
                WRITE(6,33) EKEV(J),EKEV(K),(SPECT(J,I),I=1,8)
         33     FORMAT(' I ',2F7.2,1P8E14.4,'  I')
         34     CONTINUE
                WRITE(6,38)
                WRITE(6,39) EKEV(1),EKEV(KK),TFLUX
                WRITE(6,35) ISPEC
         39     FORMAT('0',//' TOTAL INTEGRATED FLUX BETWEEN',F7.2,' AND',F7.2,
```

```
                    1'KEV    IN UNITS OF XRAYS/(CM**2*SEC)   IS  ',1PE14.5//)
0067         35     FORMAT('0',///' END OF PROCESSING FOR SPECTRUM ',I2///)
0068                GO TO 100
0069        101      CONTINUE
0070                WRITE(6,36)
0071         36     FORMAT('0',//////' COMPLETION OF UNFOLDING AND LIFTING OF SPECTRA
                   1   '//////)
0072                STOP
0073                END
```

```
      SUBROUTINE GAUS(NBINS,XKEV,XKEVA,LMDA,XSPEC1,SIGPAR)
C-----GAUSSIAN UNFOLDING OF XRAY SPECTRUM.
      REAL XKEV(51),A1(50,50),LMDA(51),XSPEC1(50),XSPEC2(50)
      REAL XSPEC3(50),XKEVA(50),SIGPAR(3)
      SQPI=1.772454
      DO 14 J=1,NBINS
      K=J+1
      DO 14 I=1,NBINS
      L=I+1
      XHIGH=XKEV(K)
      XLOW=XKEV(J)
      DE=XHIGH-XLOW
      IF (I-J) 41,43,42
   41 XMEAN=XKEV(L)
      GO TO 15
   42 XMEAN=XKEV(I)
   15 XLMDA=LMDA(I)
      A1(J,I)=SQPI*XLMDA*GAUSP(XLOW,XHIGH,XMEAN,XLMDA)/DE
      GO TO 14
   43 A1(J,I)=1.0
   14 CONTINUE
C-----LIMIT EXTRAPOLATION CORRECTION
C-----(MORE PRECISION REQ FOR SMALLER E BINING)
      DE=XKEV(2)-XKEV(1)
      X4=XKEVA(1)-DE
      SZERO=XTRPOL(XKEVA(3),XKEVA(2),XKEVA(1),X4,XSPEC1(3),
     1XSPEC1(2),XSPEC1(1))
      XLMDA=SIGF(X4,SIGPAR(1),SIGPAR(2),SIGPAR(3))/2.0
      SALPHA=SZERO*DE/(DE+SQPI*XLMDA)
      XMEAN=XKEV(1)
      XLOW=XKEV(1)
      XHIGH=XKEV(2)
      SCORR=SALPHA*SQPI*XLMDA*GAUSP(XLOW,XHIGH,XMEAN,XLMDA)/DE
      WRITE(6,51) SZERO,SALPHA,SCORR
   51 FORMAT('0SZERO,SALPHA,SCORR=    ',3E14.4)
      XSPEC1(1)=XSPEC1(1)-SCORR
      NK2=NBINS-2
      NK1=NBINS-1
      NN1=NBINS+1
      DE=XKEV(NN1)-XKEV(NBINS)
      X4=XKEVA(NBINS)+DE
      SZERO=XTRPOL(XKEVA(NK2),XKEVA(NK1),XKEVA(NBINS),X4,XSPEC1(NK2),
     1XSPEC1(NK1),XSPEC1(NBINS))
      XLMDA=SIGF(X4,SIGPAR(1),SIGPAR(2),SIGPAR(3))/2.0
      SALPHA=SZERO*DE/(DE+SQPI*XLMDA)
      XMEAN=XKEV(NBINS)
      XLOW=XKEV(NBINS)
      XHIGH=XKEV(NN1)
      SCORR=SALPHA*SQPI*XLMDA*GAUSP(XLOW,XHIGH,XMEAN,XLMDA)/DE
      WRITE(6,51) SZERO,SALPHA,SCORR
      XSPEC1(NBINS)=XSPEC1(NBINS)-SCORR
C-----NOW SOLVE MATRIX OF CONVOLUTION COEFF. FOR S ALPHA.
      WRITE(6,30)
   30 FORMAT('0',///' PROBABILITY CONVOLUTION MATRIX'/)
      DO 16 I=1,NBINS
      WRITE(6,31) (A1(I,J),J=1,NBINS)
   31 FORMAT(10F7.3)
   16 XSPEC2(I)=XSPEC1(I)
```

```
      CALL RSIMQ(50,NBINS,A1,XSPEC2,0)
      CONTINUE
      DO 17 I=1,NBINS
      K=I+1
      XSPEC3(I)=XSPEC2(I)*(1.0+SQPI*LMDA(I)/(XKEV(K)-XKEV(I)))
 17   CONTINUE
      WRITE(6,18)
 18   FORMAT('0ENERGY BIN    FOLDED SPECT  ALPHA SPECT   UNFOLDED SP'/)
      DO 19 I=1,NBINS
      K=I+1
 19   WRITE(6,20) XKEV(I),XKEV(K),XSPEC1(I),XSPEC2(I),XSPEC3(I)
 20   FORMAT(2F7.2,1P3E14.4/)
      WRITE(6,21)
 21   FORMAT('0',//////' END OF GAUSSIAN UNFOLDING '////)
      DO 22 I=1,NBINS
 22   XSPEC1(I)=XSPEC3(I)
      RETURN
      END
```

```
0001                SUBROUTINE RSIMQ(NDIM, NORDER, COEFF, RHS, IERR)
              C
0002                REAL COEFF, RHS, BIGC, SAVE, TOL, ABS
0003                INTEGER NORDER, NDIM, I, J, K, IMAX, JP1, JJ, NM1
              C
0004                DIMENSION COEFF(NDIM, NORDER), RHS(NORDER)
              C
              C   CHECK FOR ARGUMENT ERRORS.
0005                IF (NDIM .GE. NORDER .AND. NORDER .GT. 0) GO TO 10
0006                IERR = 2
0007                WRITE (6, 1001) NDIM, NORDER
0008                RETURN
              C
0009             10 TOL = 0.0E0
0010                IERR = 0
              C
              C   DO FORWARD ELIMINATION, WITH PARTIAL PIVOTING.
0011                DO 70 J = 1, NORDER
              C
              C   CHOOSE LARGEST ELEMENT REMAINING IN THIS COLUMN.
0012                   BIGC = 0.0E0
0013                   DO 20 I = J, NORDER
0014                      IF (ABS(BIGC) .GE. ABS(COEFF(I, J))) GO TO 20
0015                      BIGC = COEFF(I, J)
0016                      IMAX = I
0017             20    CONTINUE
              C
              C   IF ALL ELEMENTS HAVE MAGNITUDES LESS THAN OR EQUAL TO TOL, THEN
              C   MATRIX IS SINGULAR.
0018                   IF (ABS(BIGC) .GT. TOL) GO TO 30
0019                   IERR = 1
0020                   WRITE (6, 1002)
0021                   RETURN
              C
              C   INTERCHANGE ROWS IF NECESSARY, AND DIVIDE NEW CURRENT ROW BY
              C   PIVOT ELEMENT.
0022             30    DO 40 K = J, NORDER
0023                      SAVE = COEFF(IMAX, K)
0024                      COEFF(IMAX, K) = COEFF(J, K)
0025                      COEFF(J, K) = SAVE / BIGC
0026             40    CONTINUE
              C
              C   DO THE SAME FOR THE RIGHT-HAND SIDE.
0027                   SAVE = RHS(IMAX)
0028                   RHS(IMAX) = RHS(J)
0029                   RHS(J) = SAVE / BIGC
              C
              C   SUBTRACT MULTIPLES OF THIS ROW FROM ANY REMAINING ROWS TO MAKE
              C   LEADING COEFFICIENTS VANISH.
0030                   IF (J .GE. NORDER) GO TO 80
              C
0031                   JP1 = J + 1
0032                   DO 60 I = JP1, NORDER
0033                      SAVE = COEFF(I, J)
0034                      DO 50 K = JP1, NORDER
0035             50          COEFF(I, K) = COEFF(I, K) - SAVE * COEFF(J, K)
0036                      RHS(I) = RHS(I) - SAVE * RHS(J)
0037             60    CONTINUE
```

```
0038            70 CONTINUE
              C
              C   NOW FIND ELEMENTS OF SOLUTION VECTOR IN REVERSE ORDER BY DIRECT
              C   SUBSTITUTION.
0039            80 NM1 = NORDER - 1
0040               NP1 = NORDER + 1
0041               DO 100 JJ = 1, NM1
0042                  J = NORDER - JJ
0043                  JP1 = J + 1
0044                  DO 90 KK = 1, JJ
0045                     K = NP1 - KK
0046                     RHS(J) = RHS(J) - COEFF(J, K) * RHS(K)
0047            90    CONTINUE
0048           100 CONTINUE
              C
0049               RETURN
              C
0050          1001 FORMAT(23H RSIMQ   ARGUMENT ERROR, 2I11)
0051          1002 FORMAT(32H RSIMQ   EQUATIONS ARE SINGULAR.)
0052               END
```

```
0001            SUBROUTINE ESCAPE(XKEV,TSPECT,NBINS)
          C-----ESCAPE CORRECTION ON ENTIRE EXPANDED SPECTRUM
          C     RETURNS NEW SPECTRUM BY CLOBBERING TSPECT
0002            REAL XKEV(51),TSPECT(50),FSPECT(300)
0003            INTEGER IKEV(51)
0004            KK=NBINS+1
0005            DO 10 I=1,KK
0006      10    IKEV(I)=IFIX(XKEV(I))
0007            LD=IKEV(KK)-IKEV(1)
0008            ICOUNT=NBINS
0009            DO 20 I=1,LD
0010            N=LD-I+IKEV(1)
0011            IF (N.LT.IKEV(ICOUNT)) ICOUNT=ICOUNT-1
0012            IC1=ICOUNT+1
0013            FSPECT(N)=TSPECT(ICOUNT)/(IKEV(IC1)-IKEV(ICOUNT))
          C.....WRITE(6,101) ICOUNT,IKEV(ICOUNT),TSPECT(ICOUNT),N,FSPECT(N)
0014      20    CONTINUE
0015            DO 30 I=1,LD
0016            N=LD-I+IKEV(1)
0017            N29=N-29
0018            ESC=ESCR(FLOAT(N))
0019            IF (N29.GE.IKEV(1)) FSPECT(N29)=FSPECT(N29)/(1+ESC*FSPECT(N)/FSPEC
               1T(N29))
0020            FSPECT(N)=FSPECT(N)/(1-ESC)
0021      30    CONTINUE
0022            DO 40 I=1,NBINS
0023      40    TSPECT(I)=0.0
0024            ICOUNT=NBINS
0025            DO 50 I=1,LD
0026            N=LD-I+IKEV(1)
0027            IF (N.LT.IKEV(ICOUNT)) ICOUNT=ICOUNT-1
0028            TSPECT(ICOUNT)=TSPECT(ICOUNT)+FSPECT(N)
          C.....WRITE(6,101) ICOUNT,IKEV(ICOUNT),TSPECT(ICOUNT),N,FSPECT(N)
0029      50    CONTINUE
0030      101   FORMAT(' ICOUNT,IKEV(ICOUNT),TSPECT(ICOUNT),N,FSPECT(N) = ',
               *2I4,E14.4,I4,E14.4)
0031            RETURN
0032            DEBUG SUBCHK
0033            END
```

```
0001            SUBROUTINE EPSD
          C-----EFFICIENCY OF PULSE HEIGHT DISCRIMINATOR
          C     THIS ENTRY READS THE EFFICIENCY TABLE
0002            DIMENSION PSD(50,7),CDTX(50),CDTY(50),EX(7),EY(7)
0003            READ(5,10) NTIMES
0004      10    FORMAT(I2)
0005            DO 20 I=1,NTIMES
0006      20    READ(5,30) CDTX(I),(PSD(I,J),J=1,7)
0007      30    FORMAT(F10.0,7F10.3)
0008            RETURN
0009            ENTRY EFFPSD(EFF,T,E,EX)
          C-----INTERPOLATES EFFICIENCY TABLE FOR A GIVEN TIME AND ENERGY
          C     WRITE(6,81) EFF,T,E,(EX(I),I=1,7)
0010      81    FORMAT('0EFF,T,E,EX= ',10F10.2)
0011            DO 50 J=1,7
0012            DO 40 I=1,NTIMES
0013      40    CDTY(I)=PSD(I,J)
0014      50    EY(J)=FINTRP(T,NTIMES,CDTX,CDTY)
0015            EFF=FINTRP(E,7,EX,EY)
          C     WRITE(6,82) EFF,(EY(I),I=1,7),(CDTX(I),CDTY(I),I=1,NTIMES)
0016      82    FORMAT('0EFF,EY,CDTX,CDTY= ',F7.2,/7F7.2,/10F10.2,/10F10.2,/
               * 10F10.2,/10F10.2/)
0017            RETURN
0018            END
```

```
FORTRAN IV G LEVEL  19                    GAUSP              DATE = 75126           21/55/37

 0001                 FUNCTION GAUSP(X1,X2,XMEAN,SIGMA)
             C-----COMPUTES THE INTEGRAL UNDER A NORMALIZED GAUSSIAN DISTRIBUTION
             C        APPROX. ACCURATE TO  SIX  DIGITS. X1=LOWER AND X2=UPPER INTEGRATION
             C        LIMITS IN TERMS OF X COORDINATE, NOT SIGMA UNITS
 0002                 REAL BB(5)/.31938153, -.35656378, 1.7814779, -1.8212560, 1.3302744
                    1/
 0003                 REAL XX(2),RR(2),PP(2),EE(2)
 0004                 XX(1)=(X1-XMEAN)/SIGMA
 0005                 XX(2)=(X2-XMEAN)/SIGMA
 0006                 DO 30 I=1,2
 0007                 PP(I)=1./(1.+.2316419*ABS(XX(I)))
 0008                 T=1.0
 0009                 RR(I)=0.0
 0010                 DO 10 J=1,5
 0011                 T=T*PP(I)
 0012        10       RR(I)=RR(I)+T*BB(J)
 0013                 IF(XX(I).LT.0.0) RR(I)=1.0-RR(I)
 0014                 EE(I)=0.0
 0015        30       IF(XX(I).LT.10.0.AND.XX(I).GT.-10.0) EE(I)=EXP(-XX(I)*XX(I)/2)
 0016                 GAUSP=ABS((RR(2)*EE(2)-RR(1)*EE(1))/2.506628)
             C        WRITE (6,20) GAUSP,X1,X2,XMEAN,SIGMA
 0017        20       FORMAT(' GAUSP,X1,X2,MEAN,SIGMA= ',5F10.4)
             C        WRITE(6,21) (XX(I),RR(I),PP(I),EE(I),I=1,2)
 0018        21       FORMAT(10E12.3)
 0019                 RETURN
 0020                 END
```

```
FORTRAN IV G LEVEL  19                    ESCR               DATE = 75126           21/55/37

 0001                 FUNCTION ESCR(E)
             C-----APPROXIMATE ESCAPE PROBABILITY FOR X-RAYS FROM IODINE K FLOURESCENCE
             C        VIA FRONT FACE OF 3 MM NAI CRYSTAL
 0002                 IF(E.LE.33.) GO TO 1
 0003                 IF(E.GT.33..AND.E.LE.50.) GO TO 2
 0004                 IF(E.GT.50..AND.E.LE.80.) GO TO 3
 0005                 IF(E.GT.80.) ESCR=.055
 0006                 RETURN
 0007        1        ESCR=0.
 0008                 RETURN
 0009        2        ESCR=.27-((E-33.)/25.)*.21
 0010                 RETURN
 0011        3        ESCR=.14-((E-50.)/25.)*.08
 0012                 RETURN
 0013                 END
```

```
FORTRAN IV G LEVEL  19                  XTRPOL              DATE = 75126          21/55/37

 0001              FUNCTION XTRPOL(X1,X2,X3,X4,S1,S2,S3)
             C-----APPROXIMATE EXTRAPOLATION FOR DETECTED SPECTRUM FUNCTION.
 0002              SLOPE1=(S2-S1)/(X2-X1)
 0003              SLOPE2=(S3-S2)/(X3-X2)
 0004              SLOPE3=0
 0005              IF(SLOPE1.EQ..0) GO TO 5
 0006              IF (SLOPE1.GT.0.0 .AND. SLOPE2.GT.0.0) GO TO 1
 0007              IF (SLOPE1.LT.0.0 .AND. SLOPE2.LT.0.0) GO TO 1
 0008              SLOPE3=SLOPE2-SLOPE1
 0009              GO TO 5
 0010        1     SLOPE3=SLOPE2*SLOPE2/SLOPE1
 0011              IF(ABS(SLOPE3).GT.ABS(SLOPE2)) SLOPE3=SLOPE2
 0012        5     XTRPOL=SLOPE3*(X4-X3)+S3
 0013              WRITE(6,10) SLOPE1,SLOPE2,SLOPE3,XTRPOL
 0014        10    FORMAT('0SLOPE1,SLOPE2,SLOPE3,XTRPOL =   ',4E14.6/)
 0015              RETURN
 0016              END
```

```
FORTRAN IV G LEVEL  19                  FINTRP              DATE = 75126          21/55/37

 0001              FUNCTION FINTRP(X,NVALS,XVALS,YVALS)
             C-----INTERPOLATES TABULATED FUNCTION, XVALS AND F(XVALS) = YVALS
             C     TO CALCULATE F(X). LINEAR EXTRAPOLATION IF X OUTSIDE TABULATED RANGE.
 0002              DIMENSION XVALS(50),YVALS(50)
 0003              IF(X.LE.XVALS(1)) GO TO 20
 0004              IF(X.GE.XVALS(NVALS)) GO TO 30
 0005              N=1
 0006        10    N1=N
 0007              N=N+1
 0008              IF(N.GT.NVALS) GO TO 30
 0009              IF(X.GT.XVALS(N)) GO TO 10
 0010              FINTRP=YVALS(N1)+(X-XVALS(N1))*(YVALS(N)-YVALS(N1))/(XVALS(N)-
                  1 XVALS(N1))
 0011              GO TO 40
 0012        20    FINTRP=YVALS(1)-(XVALS(1)-X)*(YVALS(2)-YVALS(1))/(XVALS(2)-
                  1 XVALS(1))
 0013              GO TO 40
 0014        30    FINTRP=YVALS(NVALS)+(X-XVALS(NVALS))*(YVALS(NVALS)-YVALS(NVALS-1))
                  1 /(XVALS(NVALS)-XVALS(NVALS-1))
 0015        40    CONTINUE
             C     WRITE(6,81) FINTRP,X,NVALS
 0016        81    FORMAT('0 INTERP,X,NVALS= ',2F10.2,I3)
             C     WRITE (6,82) (XVALS(I),YVALS(I),I=1,NVALS)
 0017        82    FORMAT(' XVALS,YVALS= ',10F10.2)
 0018              RETURN
 0019              DEBUG SUBCHK
 0020              END
```

```
FORTRAN IV G LEVEL  19                    TRAIR                DATE = 75126          21/55/37

                   FUNCTION TRAIR(THAIR,E)
             C-----PROBABILITY OF TRANSMISSION THROUGH ATMOSPHERE
                   TRAIR=EXP(-(5.30*(10./E)**2.90+.16)*THAIR)
                   RETURN
                   END
```

```
FORTRAN IV G LEVEL  19                    TRINS                DATE = 75126          21/55/37

                   FUNCTION TRINS(EE)
             C-----PROBABILITY OF TRANSMISSION THRU STYROFOAM LAYER (JUNE, 1974)
                   TRINS=EXP(-1.0*(8.6/EE)**2.65)
                   RETURN
                   END
```

```
FORTRAN IV G LEVEL  19                    TRNAI                DATE = 75126          21/55/37

                   FUNCTION TRNAI(THNAI,E)
             C-----PROBABILITY OF TRANSMISSION THROUGH NAI CRYSTAL
                   IF(E-33.0) 1,1,2
              1    A=5.8
                   GO TO 3
              2    A=28.0
              3    TRNAI=EXP(-THNAI*(A*(33.0/E)**2.65))
                   RETURN
                   END
```

```
FORTRAN IV G LEVEL  19                    SIGF                 DATE = 75126          21/55/37

                   FUNCTION SIGF(E,A,B,C)
             C-----GIVES SIGMA FOR GAUSSIAN RESPONSE FUNCTION -- EMPIRICAL FORMULA
                   SIGF = (A*E + B*SQRT(E) + C)
                   RETURN
                   END
```

```
FORTRAN IV G LEVEL  19                    EFFEL                DATE = 75126          21/55/37

                   FUNCTION EFFEL(E)
             C-----EFFICIENCY OF ELECTRONICS ON SCALE 1 TO 0
                   EFFEL=0.94
                   RETURN
                   END
```

BIBLIOGRAPHY

1) Ricker, G. R., Scheepmaker, A., et al, Astrophysical J. V 197, pp. L83-87, 1975.

2) Clark, G. W., Lewin, W. H. G., Smith, W. B., Astrophysical J. V 151, pp. 21-32, 1968.

3) Rose, W. K., Astrophysics. Holt, Rinehart and Winston, 1973.

4) Lloyd, K. H., American J. Physics, V 37, pp. 329-330, 1969.

5) Proposal to the National Science Foundation for x-ray balloon observations. Center for Space Research, M.I.T., 1974.

6) Hoyng, P., Stevens, G. A., Astrophysics Sp. Sci., V 27, pp. 307-321, 1974.

7) Handbook of Mathematical Functions, Abramowitz and Stegun (eds.) U.S. Department of Commerce, 1964.

8) Laros, J. G., Matteson, J. L., Pelling, R. M., Nature Physical Sci., V 246, pp. 109-111, 1973.